Asian Journal of Research and Reviews in Physics

Volume 6, Issue 4, Page 7-17, 2022; Article no.AJR2P.88040
ISSN: 2582-5992

Calculation of Cohesive Energies of 3-D Bismuth Selenide (Bi_2Se_3) and Bismuth Antimony BiSb Topological Insulators: DFT Study

E. C. Hemba [a], T. J. Ikyumbur [b*], E. A. Trisma [a], F. Gbaorun [b] and F. Aungwa [c]

[a] Department of Physics, Federal College of Education, Pankshin, Plateau State, Nigeria.
[b] Department of Physics, Benue State University, Makurdi, Benue State, Nigeria.
[c] Department of Physics, Nigeria Defence Academy, Kaduna, Kaduna State, Nigeria.

Authors' contributions

This work was carried out in collaboration among all authors. All authors read and approved the final manuscript.

Article Information

DOI: 10.9734/AJR2P/2022/v6i4124

Open Peer Review History:
This journal follows the Advanced Open Peer Review policy. Identity of the Reviewers, Editor(s) and additional Reviewers, peer review comments, different versions of the manuscript, comments of the editors, etc are available here: https://www.sdiarticle5.com/review-history/88040

Original Research Article

Received: 10/04/2022
Accepted: 18/06/2022
Published: 23/12/2022

ABSTRACT

The cohesive energies of 3-dimensional (3-D) topological insulators bismuth antimony (BiSb) and bismuth selenide (Bi_2Se_3) were calculated. The Fritz Haber Institute Ab-initio molecular simulations (FHI-aims) code was employed for this calculation. The output files of the FHI-aims code were used during the computation and the total energies at each number of iterations for single free atoms and bulk were then calculated. The results from this work revealed that bismuth atom becomes stable at 3rd iteration meanwhile both selenium and antimony atoms gain stability at the 5th iteration. The results also showed that bismuth antimony acquire stability at the 3rd iteration and bismuth selenide gain stability at 9th iteration. This implies that among the free atoms studied in this work bismuth atom is more stable and for the bulk bismuth antimony is more stable. The cohesive energies of BiSb and Bi_2Se_3 were calculated using the optimized parameters. The results obtained

**Corresponding author: E-mail: ikyumburtj@yahoo.com, jikyumbur@bsum.edu.ng;*

from the calculation of the cohesive energies in this work were 1.02eV and 1.76eV for BiSb and Bi_2Se_3 respectively. This results compared reasonably well with experimental results and have little percentage errors of 1.30% for bismuth antimony and 29.55% for bismuth selenide. The deviation observed in this work may be due to the DFT calculation of the solid rather than the atoms themselves.

Keywords: Cohesive energies; topological insulators; FHI-aims; bismuth selenide (Bi2Se3); bismuth antimony (BiSb) and DFT.

1. INTRODUCTION

Topological is the newest electronic phase discovered recently. Hitherto, the electrical conductor, insulator, semiconductor, and the superconductor were the first electronic phase of matter to be known. "The most exciting thing about this new electronic phase is the behaviour. Materials in this new phase behave strangely. The topological insulator can insulate on the inside but conduct on the outside. This new electronic phase of matter are said to be materials with non-trivial symmetry protected topological order that behaves as an insulator in its interior but whose surface contains conducting states" [1]. The materials in this phase are unique in the sense that the conducting electrons arrange themselves into spin-up electrons travelling in one direction, and spin-down electrons travelling in the other. This imply that electrons can only move along the surface of the material.

"The conducting surface possessed by topological insulator is however not unique to them only, ordinary band insulators also support conductivity on the surface states. The only distinctive thing about topological insulators is that their surface states are symmetry protected by particle number of conservation and time reversal symmetry" [2-4].

"The electronic band structure resembles an ordinary band insulator in the bulk of the non-interacting topological insulator, with the Femi level falling between the conduction and valence bands. This implies that, on the surface of the topological insulator there are special states that fall within the bulk energy gap and allow surface metallic conduction. It has established that carriers in these surface states have their spin locked at a right-angle to their momentum (spin-momentum locking)" [5]. "At a given energy the only other available electronic states have different spin, so the U-turn scattering is strongly suppressed and conduction on the surface is highly metallic. Non-interacting topological insulators are characterized by an index known as the Z_2 topological invariants similar to the genus in topology" [6].

"The protected conducting states in the surface are required by time-reversal symmetry and the band structure of the material" [7]. "This shows that states cannot be removed by surface passivation if it does not break the time-reversal symmetry, which does not happen with potential or spin-orbit scattering but happens in case of true magnetic impurities such as spin- scattering" [8].

"Topological insulators have a rather unusual history because unlike almost every other exotic phase of matter, topological insulators were characterized theoretically before being discovered experimentally. This new electronic phase of matter was discovered in 2007 experimentally. The first realized 3D topological state (symmetry-protected surface states) discovered experimentally in bismuth-antimony (BiSb)" [9]. "Shortly thereafter symmetry-protected surface states were discovered in pure antimony (Sb), bismuth selenide (Bi_2Se_3), bismuth telluride (Bi_2Te_3) and antimony telluride (Sb_2Te_3)" [10].

"This research work was initiated due to the importance of BiSb and Bi_2Se_3 in the modern technology. Today, many semiconductors within the large family of Heusler materials are now believed to exhibit topological surface states" [11]. "In some of these materials Femi level actually falls in either the conduction or valence bands due to naturally occurring defects and must be pushed into the bulk gap by doping or gating" [12].

"This recent discovery did draw the attention of many Solid-State Physicists. A related topological property known as the quantum Hall effect had already been found in 2D ribbons in the early 1980s but the discovery of the first example of a 3D topological phase reignited that earlier interest. Given that the 3D topological

insulators are fairly standard bulk semiconductors and their topological characteristics can survive to high temperatures" [13]. Other notable research on topological insulators is in energy generation of electricity by converting thermal gradients occurring naturally or from waste heat sources into useful electrical energy [14] and "Raman Spectroscopy determination of Debye temperature and atomic cohesive energy" [15]. In this work however, the cohesive energies of bismuth selenide (Bi_2Se_3) and bismuth antimony (BiSb) were calculated by the researches using density functional theory.

"Cohesive energy is amount of energy involved when a crystalline solid is formed from infinity separated atoms or the amount of energy required to separate atoms in a crystalline solid to infinite distance. In Physics however, cohesive energy means the difference between the average energy of the free atoms and that of the atoms of a solid especially a crystal. It is the quantity which determines the structure, because different possible structures would have different cohesive energies" [16]. The magnitude of cohesive energy also tells us about the stability and chemical reactivity of solids.

2. THEORETICAL FRAMEWORK

"Density Functional Theory (DFT) is a computational quantum mechanical modelling method used in Physics, Chemistry and material science to investigate the electronic structure (especially the ground state) of many-body systems, in particular atoms, molecules, and the condensed phase" [17-20]. "Applying this theory, the properties of a many-electron, which in this case is the spatially dependent electron density. DFT has been the dominant method for quantum mechanical simulation of periodic systems. In recent years it has also been adopted by quantum chemistry and is now very widely used for simulation of energy surfaces in molecules" [21].

"Traditional methods in electronic structure theory, particularly the Hatree-Fock theory and its descendants are based on the complicated many-electron wave function. The main objective of DFT is to replace the many-body electronic wave function with the electronic density as the basic quantity. Thereby making many-body wave function dependent on 3N variables, three special variables for each of the N electrons, the density is only a function of the three variables and is simpler to deal with both conceptually and practically" [22].

2.1 The Hohenberg-Kohn Theorem

The Hohenberg –Kohn (H-K) theorem states that the electrons density of any system determines all ground-state properties of the system. In this case the total ground state energy of a many-electron system is a function of the density [23-25].

The theory assumes a system of N-interacting electrons under an external potential $V(r)$. This potential is usually the coulomb potential of the nuclei. If the system has a non-degenerate ground state, it is obvious that there is only one ground state charge density that corresponds to a given $V(r)$. Hohenberg and Kohn demonstrated that there is only one external potential $V(r)$ that yields a given ground state charge density $n(r)$.

Hohenberg and Kohn demonstrated that for many-electron Hamiltonian $H = T + U + V,$ with ground state wave function, ψ. Whereas T, U, V are the kinetic energy, electron-electron interaction and the external potential respectively. The charge density $n(r)$ is defined by:

$$n(r) = N \int \left|\psi\left(r_{1,} r_{2,} r_3 \ldots r_N\right)\right|^2 dr^2 . dr^N \quad (1)$$

Differentiating the Hamiltonian $H' = T' + U' + V'$. The potential V and its derivatives V' does not differ by a constant. That is to say $V - V' \neq$ constant with the ground state wave function ψ. Assuming that the ground state charge densities are the same (i.e. $n[V] = n'[V']$. The following inequality will hold [26,27].

$$E < \langle\psi'|H|\psi'\rangle = \langle\psi'|H'|\psi'\rangle + \langle\psi'|H - H'|\psi'\rangle \quad (2)$$

$$E < E' + \langle\psi'|T + U + V - T - U - V'|\psi' \quad (3)$$

This implies that:

$$E < E' + \int n(r)\{V - V'\}dr \quad (4)$$

The reverse relation of equation (4) will now be

$$E' < E - \int n(r)\{V - V'\}\, dr \quad (5)$$

Adding equation (4) and equation (5) gives

$$E + E' < E' + E \text{ Contradiction!} \quad (6)$$

The inequality in the above equation is strict because ψ and ψ' are different, being eigen state of different Hamiltonian. Reversing the prime and unprime quantities, one obtains an inconsistent result. This showed that no two potentials can have the same density. The first Hohenberg-Kohn theorem that has a straight forward consequence is that of the ground state energy E. The theory also uniquely determined by the ground state charge density. It is a function of density $E[n(r)]$ [28] and can be written mathematically as:

$$E[n(r)] = (\psi|T + U + V|\psi) = (\psi[T + U]|\psi) + (\psi|V|\psi) = F[n(r)] + \int n(r)V(r)dr \quad (7)$$

$F[n(r)]$ is a universal function of the charge density $n(r)$ but not of $V(r)$ also known as the H-K functional [29]. For this functional variation principle holds and the ground state energy is minimized by the ground state charge density. In this way, the DFT exactly reduces the N-body problem to determine a 3-dimensional function $n(r)$ which minimizes a functional $E[n(r)]$.

2.2 The Kohn-Sham (KS) Equations

Kohn and Sham in 1965 reformulated the problem in a more familiar form and opened up the practical application of DFT. Here, the system of interacting electrons is mapped onto a fictitious system of non-interacting electrons having the same charge density $n(r)$. K-S represented the ground state energy charge density by a system of non-interacting electrons over one-electron orbitals also known as K-S orbitals ψ_i as:

$$n(r) = 2\sum_i |\psi_i(r)|^2 \quad (8)$$

Where i runs from 1 to $\frac{N}{2}$. If we assume a double occupancy of all states and Kohn-Sham orbitals are solutions to the Schrodinger equation:

$$E_i\psi_i(r) = \left(-\frac{\hbar^2}{2m}\nabla^2 + V_{ks}(r)\right)\psi_i(r) \quad (9)$$

Where m is the electron mass. Obeying orthogonality constraints we write:

$$\int \psi_i^*(r)\psi_j(r)dr = \delta_{ij} \quad (10)$$

The existence of a unique potential $V_{ks}(r)$ having $n(r)$ as its ground state charge density is a consequence of the Hohenberg and Kohn theorem which holds irrespective of the form of the electron-electron interaction U.

3. METHOD FOR CALCULATION OF COHESIVE ENERGIES

"All materials system essentially consists of electrons and nuclear charge and it is due to electron and its interaction with other electrons which results in various mechanical, electronic and magnetic properties. In order to define electron and their interaction Schrodinger equation is the best tool [30]. If Schrodinger equation of many electron problems can be solved accurately and efficiently then almost any property of the materials can be determined accurately but unfortunately there is neither an accurately nor efficient method to solve these problems". "There are various methods developed to solve Schrodinger equation. Relatively simple system as Hydrogen atom and H_2^+ could be solved analytically. To solve relatively complex system, methods like Nearly free electron method and Tight binding method have been developed. These methods are not accurate as we have to take a lot approximation to simplify the problem [31]. After this grand success many methods have been developed to compute various properties such as Quantum Chemistry (Hartree-Fock), Quantum Monte Carlo, Perturbation theory and Density Functional Theory (DFT). In this research work DFT the most successful of them all were used. By successful we mean it is best combination of accuracy and efficiency".

To illustrate the basic idea behind DFT, we first formulate the problem of one electron as a density functional problem. We know that the ground state energy can be written as a density functional instead of as wavefunction functional. This functional is:

$$E[n] = \frac{1}{8}\int d^3r \frac{|\nabla n|^2}{n} + \int d^3r\, v(r)n(r) \quad (11)$$

In any number of dimensions, we must minimize it, subject to the constraint that $\int d^3 \mathrm{rn}(r) = 1$.

Using Lagrange multipliers, we construct the auxiliary functional:

$$H[n] = E[n] - \mu N \quad (12)$$

where$N = \int d^3 \mathrm{rn}(r)$. Minimizing this yields:

$$\frac{\delta H}{\delta n(r)} = \frac{\delta T^{\mathrm{VW}}}{\delta n(r)} + v(r) - \mu = 0 \quad (13)$$

Using the derivation of a semi-local functional, we find the Schrodinger equation for the density as:

$$\left(-\frac{\nabla^2}{4}+\frac{|\nabla n|^2}{8n^2}+v(r)n(r)\right)=\mu n(r) \qquad (14)$$

with boundary conditions that $n(r)$and$\nabla n(r)\to 0$ at the edges. We can identify the Lagrange multiplier by integrating both sides over all space at the solution. Since the integral of any Laplacian vanishes (with the given boundary conditions), we see that $\mu = E$.

It is self-evident that the external potential in principle determines all the properties of the system; this is the normal approach to quantum mechanical problems, by solving the Schrödinger equation for the eigenstates of the system.

The first principles of Hohenberg and Kohn (H-K) theorem demonstrates that the ground state properties of a many-electron system are uniquely determined by an electron density that depends on only three spatial co-ordinates which reduces our problem to 3 spatial co-ordinates from 3N spatial co-ordinates for N body problem because of the use of density functional. The N particle system of interacting particles with 3N degrees of freedom is reduced to a significantly more tractable problem, which deals with a function (density) of only three variables. The many-body effects incorporated in the exchange-correlation potential are typically approximated within either the local density approximation or the generalized gradient approximation. The formulation applies to any system of interacting particles in an external potential $V_{ext}(r)$including any problem of electrons and fixed nuclei, where the Hamiltonian can be written as:

$$H=-\sum_i\frac{\hbar^2}{2m_e}\nabla_{r_i}^2+\sum_i V_{\text{ext}}(r_i)+\frac{e^2}{2}\sum_{i\neq j}\frac{1}{|r_i-r_j|}+\sum_{i\neq j}\frac{Z_iZ_je^2}{|R_i-R_j|} \qquad (15)$$

The first term in this equation corresponds to the kinetic energy of the interacting electrons, the second term is the external potential acting on the electrons due to the ions, the third term is the electron Coulomb interaction, and the last term is the interaction energy of the nuclei. Since the Hamiltonian is thus fully determined (except for a constant shift of the energy), it follows that all properties of the system can be found given only the ground state density $n(r)$. This result allowed Hohenberg and Kohn to prove the existence of an energy functional of the density $E[n(r)]$, which assumes its minimum value for the correct ground state density.

$$E[n(r)]=\int V_{ext}(r)n(r)dr+F[n(r)] \qquad (16)$$

The minimization of energy functional $E[n(r)]$ with respect to the charge density with the constraint of fixed number of electrons gives the ground state energy and the ground state charge density from which all other physical properties can be extracted. However in spite of the universality of $F[n(r)]$ no explicit expressions for this functional are known to date. In 1965, Kohn and Sham readdressed the problem of minimizing the Hohenberg-Kohn density functional (Eq. 16) directly with an improved strategy that maps the original interacting problem into an auxiliary non-interacting one [31]. This is achieved by expressing the charge density $n(r)$ as:

$$n(r)=\sum_i|\psi_i(r)| \qquad (17)$$

Where $\psi_i's$ are the single-particle wavefunctions for the non-interacting electron gas with ground state charge density $n(r)$, and the sum is over all occupied singleparticle states.

The $F[n(r)]$ functional is now expressed as:

$$F[n(r)]=T_s[n(r)]+\frac{e^2}{2}\int\frac{n(r)n(r')}{|r-r'|}drdr'+E_{xc}[n(r)] \qquad (18)$$

where the first term corresponds to the kinetic energy of a non-interacting electron gas at the same density $n(r)$, the second term is the classical Coulomb interaction energy (the Hartree term), and the last term $E_{XC}[n(r)]$ represents the quantum mechanical exchange-correlation energy. This term accounts for the differences between the non-interacting fictitious system and the real interacting one, collecting the contributions from the non-classic electrostatic interaction and the differences in their corresponding kinetic energies. The success of the Kohn–Sham approach ultimately lies in the fact that $E_{XC}[n(r)]$, which contains the many-body contributions, is a small fraction of the total energy, and although not known exactly, it can be approximated surprisingly well. The approximation is at present the strength and the limitation of DFT, providing efficient yet not exact reformulation of the quantum mechanical problem, respectively. If the energy functional defined in Eq. 16 and Eq. 18 is now varied with respect to the wave-functions $\psi_i's$ subject to the orthonormality constraint, the following set of Schrodinger equations is obtained

$$\left[\frac{-\hbar^2}{2m_e}\nabla_r^2+v_{eff}\big(r,n(r)\big)\right]\psi_i(r)=\varepsilon_i\psi_r(r) \qquad (19)$$

where the effective potential $V_{eff}(r, n(r))$ is given as

$$v_{eff}(r, n(r)) = V_{ext}(r) + e^2 \int \frac{n(r')}{|r-r'|} dr' + \frac{\delta E_{XC}[n(r)]}{\delta n(r)} \quad (20)$$

Equations 19 and 20 are called the Kohn–Sham equations and have to be solved self-consistently because of the dependence of $v_{eff}(r)$ on $n(r)$. It should be emphasized here that the Kohn–Sham procedure introduces a one-body Hamiltonian representing a single-particle electron in the mean field created by the nuclei and by all other electrons. However, it assigns no formal interpretation to the calculated orbitals and the eigenvalues. In principle, the solution of the Kohn–Sham equations would yield the exact ground state energy of the interacting electron gas problem. However, the exact exchange-correlation functional $E_{XC}[n(r)]$ for an inhomogeneous interacting electron gas is not known for general $n(r)$. To proceed further, approximations to this functional are required. The most common and extensively tested approximation is the local density approximation (LDA), in which $E_{XC}[n(r)]$ for the inhomogeneous system is constructed from a parameterized form of the exchange-correlation energy density of the homogeneous electron gas ε_{XC}^{hom} [31],

$$E_{XC}[n(r)] = \int \varepsilon_{XC}(r) n(r) dr \quad (21)$$

And

$$\frac{\delta E_{XC}[n(r)]}{\delta n(r)} = \frac{\partial [n(r) \varepsilon_{XC}(r)]}{\partial n(r)} \quad (22)$$

with $\varepsilon_{XC}(r) = \varepsilon_{XC}^{hom}[n(r)]$ .These varies the treatment of exchange correlation (LDA and GGA) to Kohn-Sham DFT given by Perdew and Wang in 1991.

"There are many computational codes of DFT among which are Abinit, Vasp, Castep, Quantum-Espresso,Dacapo, FHI-aims e.t.c. On the other hand, there are many GGA versions among which is the Perdew Burke Ernzerhof (pbe) functional [32] used in this study. The goal in DFT is to find the value of the functional F, and to do this we need to make approximations. Indeed, one of the reasons why there are so many different DFT methods is that there are multiple ways of approximating the functional" [33]. "For the purposes of this research work, FHI-aims code were been used. FHI-aims is an accurate all-electron full potential electronic structure code package for computational material science. It is simply means Fritz Haber Institute- *ab initio* molecular simulations. FHI-aims is a computer program package for computational materials science based only on quantum-mechanical first principles. The main production method is density functional theory (DFT) of HK and KS to compute the total energy and derived quantities of molecular or solid condensed matter in its electronic ground state. In addition, FHI-aims allow describing a wave-function based molecular total energy calculation based on Hartree-Fock and perturbation theory (MP2 and MP4)" [34].

To calculate the cohesive energies of bismuth selenide and bismuth antimonite, the ground state total energies of Bi, Se, and Sb for single free atom and bulk were calculated first. The energies were then converted to cohesive energies of Bi_2Se_3 and BiSb using the equation below:

$$E_{coh} = \frac{E_{bulk} - NE_{atom}}{N} = -\left[\frac{E_{bulk}}{N} - E_{atom}\right] \quad (23)$$

3.1 Procedure

"The first task is to have a Linux based operating system (0S) (Ubuntu 16.04 version installed for this research work) on a computer. FHI-aims is not supported on windows. Since FHI-aims is distributed in source code form, the next task is to compile a powerful executable program. For this, the following mandatory prerequisites are needed" [35]:

- A working FORTRAN compiler. A good example is Intel's ifort compiler.
- A compiled version of the lapack library, and a library providing optimized basic linear algebra subroutines (BLAS). Standard commercial libraries such as Intel's mkl provide both lapack and BLAS support. Having an optimized BLAS library for a specific computer system is critical for the performance of FHI-aims.

"FHI-aims requires two input files — control.in and geometry.in— located in the same directory from where the FHI-aims binary is invoked. An output file contains the basic information and result of the calculation such as the total energy, atomic forces, etc. The geometry.in file contains all information concerning the atomic structure of the system. This includes the nuclear coordinates, which are specified by the keyword atom, followed by Cartesian coordinates (in units of Å) and the descriptor of the species" [36]. "The control.in file contains all other physical and technical settings for accurate and efficient convergence of the computations. In particular, it

specifies the physical and technical settings for the equations to be solved.

The full algorithmic framework embodied in the FHI-aims computer program package is described in" [37]. "The algorithms are based on numerically tabulated atom-centered orbitals (NAOs) to capture a wide range of molecular and materials properties from quantum-mechanical first principles and all-electron/full-potential treatment that is both computationally efficient and accurate is achieved for periodic and cluster geometries on equal footing, including relaxation and *ab initio* molecular dynamics" [38].

"The programme runs interactively. You make a menu choice and change physical parameters to the system of interest. First step towards studying periodic systems with FHI-aims is to construct the periodic geometries in the FHI-aims geometry input format (geometry.in), Next, followed by setting of basic parameters in control.in for periodic calculations and finally compute total energies of different topological insulators; BiSb and Bi_2Se_3 geometries" [38].

"Geometry.in files for the BiSb and Bi_2Se_3 structures were constructed varying the lattice constants around the experimental lattice constants *a* of 4.14Å for Bi_2Se_3 and 4.38Å for BiSb At each lattice constant, if the symmetry of the system allows the ions to move, a separate geometric optimization must be performed" [38].

In setting up the geometry.in file of a periodic structure in FHI-aims, the lattice vectors of the two topological insulators as well as their atomic positions in the unit cell are specified.

You then set the output to be displayed on the screen and also saved in a file with a file name of your choice. The code is then run which displays output on the screen and also saves the result of the run in a file [39]. The total and cohesive energies of BiSb and Bi_2Se_3 were determined in the Generalized Gradient Approximation (GGA) and Local Density Approximation (LDA) using the exchange-correlation energy functional respectively. The calculation was performed by using Brillouin-zone of 12×12×12 k the SCF convergence. The graphs were plotted and analyzed from the results obtained.

4. RESULTS AND DISCUSSION

The output files of the FHI-aims code were used to obtain the results for this work. The total energies and the number of iterations for single free atoms and bulk were obtained in this work. The graphs of total energies against the number of iterations were plotted in order to obtain the optimized parameters for HCP (Bi, Se, and Sb) lattices within the local density approximation (LDA). The cohesive energies of Bi_2Se_3 and BiSb were then calculated using the optimized parameters. The results obtained from this work are presented below:

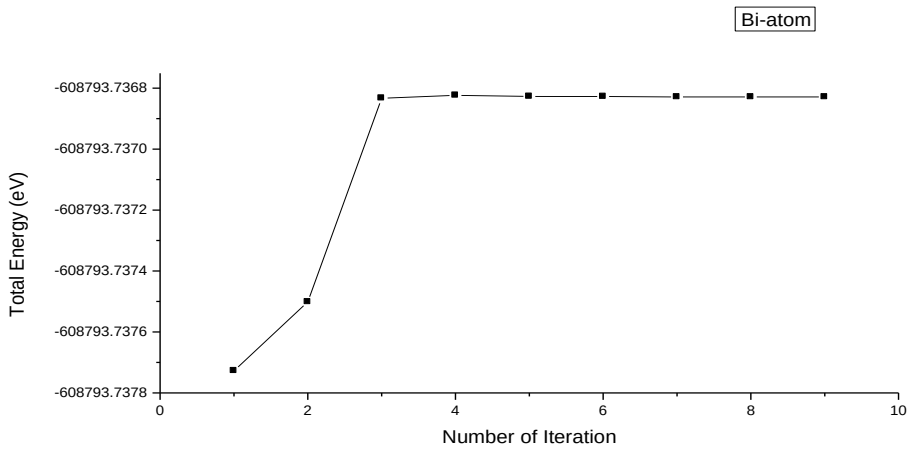

Fig. 1. Bismuth (Bi) binding curve for total energy against the number of iteration. The figure above shows that as the total energy of bismuth atom increases there is a stepwise increase in the number of iteration. The increase becomes gradual between the 2nd number of iteration until a stable energy is reached at the 3rd iteration where the stability remains fixed all through the rest of the iterations. This large negative total energy shows on the graph is due to the nature of Bi ionization energy to be too small and highly accurate in the LDA due largely to error cancellation in the attraction of the valence electron to the core of the atom of BI [40]

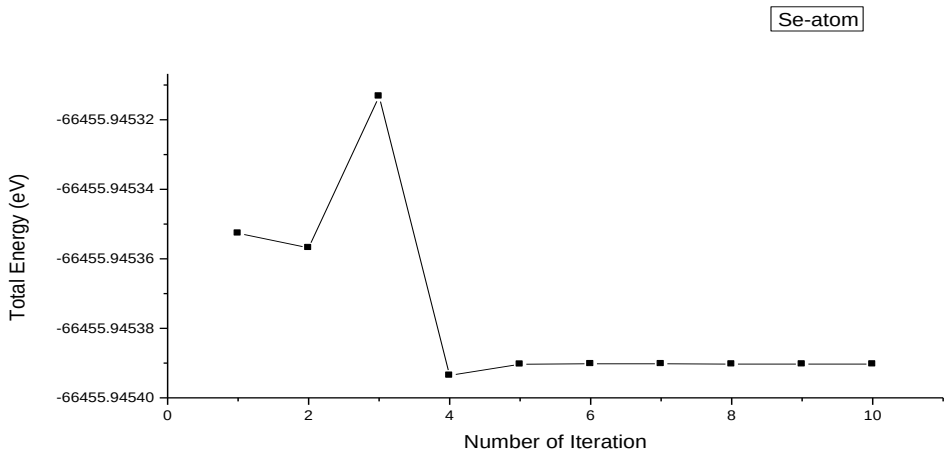

Fig. 2. Selenium (Se) binding curve for total energy against the number of iterations. The above graph showed that the total energy of selenium atom gain stability at the 5th iteration

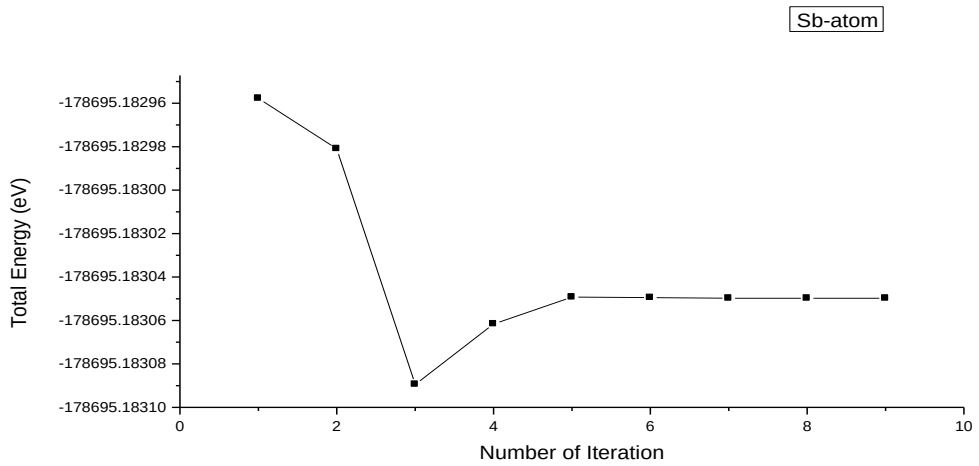

Fig. 3. Antimony (Sb) binding curve for total energy against the number of iterations. This figure showed that the total energy of antimony atom becomes a bit stable at the 5th iteration

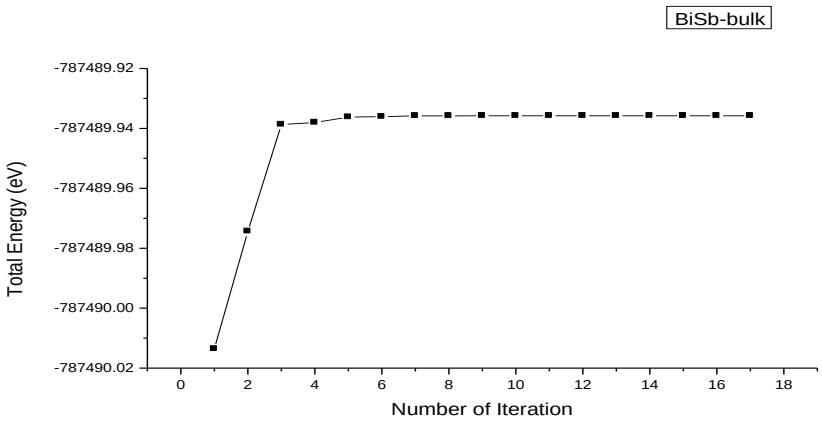

Fig. 4. Bismuth antimonite (BiSb) binding curve for total energy against the number of iterations. The binding curve for the total energy showed that bismuth antimonite (bulk) is stable at the 3th iteration

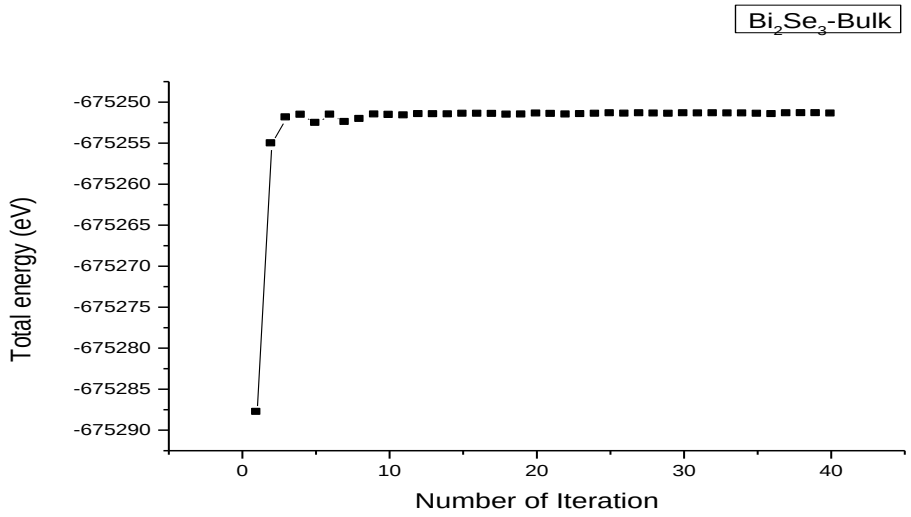

Fig. 5. Bismuth selenide (Bi_2Se_3) binding curve for total energy against the number of iterations. The total energy of antimony telluride become stable at the 9th iteration

The binding energy curve for single free atoms of Bi, Se, and Sb shown in Figs. 1 to 3 showed that the total energy of bismuth atom become stable at the 3rd iteration but selenium, and antimony atoms gain their stability at the 5th iteration. This indicates that the total energy of bismuth atom converges faster than that of Se, and Sb atoms. The total energy of bismuth atom acquire stability beginning from 3rd iteration. Meanwhile the total energy of selenium, and antimony atom begin their stability at the 5th iteration.

The cohesive energies of bismuth selenide (Bi_2Se_3) and bismuth antimonite (BiSb) were calculated using the following relations:

$$E_{coh} = E_{tot}(Bi_2) + E_{tot}(Se_3) - E_{tot}(Bi_2Se_3) \quad (24)$$

The cohesive energy of bismuth antimony was calculated to be 1.02eV and that of bismuth selenide were computed as 1.76eV. This result is in reasonable agreement with the cohesive energy obtained from T-dependent Raman shift method for bismuth selenide and bismuth antimony which is 1.09eV and 1.24eV respectively [15].

The binding curve for Bi_2Se_3 and BiSb are shown in Figs. 4 and 5 above. The binding curve in figure 5 showed that the total energy of BiSb becomes stable at 3rd iteration whereas that of Bi_2Se_3 become stable at the 9th iteration see figure 5 above. This behaviour exhibited by bismuth antimonite indicate that the alloy's total energy converges faster than that of bismuth selenide.

5. CONCLUSION

The cohesive energies of bismuth antimony and bismuth selenide were calculated within the local density approximation (LDA). The results of the total energy required for separating the condensed compound during the optimized process is found to converge faster with the $12 \times 12 \times 12$ k-grid points in the Brillioun zone of the FHI-aims code. The result presented above have confirmed a faster and more accurate study of the solid considered when compared to literature report of other studies. The values obtained are in agreement with experimental value [15] within some reasonable percentage errors. The calculated cohesive energies for bismuth antimony and bismuth selenide are observe to differ by 1.30% and 29.55% respectively. The major measure source of this deviation may come from the present DFT calculation of the solid rather than the atom.

COMPETING INTERESTS

Authors have declared that they have no known competing financial interests or non-financial interests or personal relationships that could have appeared to influence the work reported in this paper.

REFERENCES

1. Kane CL, Mele EJ. Z2 topological order and the quantum spin Hall effect. Phys Rev Lett. 1468;9(14):146802.

2. Gu Z, Wen X. Tensor-entanglement-filtering renormalization approach and symmetry-protected topological order. Phys Rev B. 2009;80(15):155131.
3. Pollmann F, Berg E, Turner AM, Oshikawa M. Symmetry Protection of Topological Phases in one –dimensional quantum spin systems. Phys Rev B. 2012;85(7):075125.
4. Chen X, Gu Z, Wen X. Classification of Gapped Symmetry Phases in 1D spin systems. Phys Rev B. 2011;83(3):035107.
5. Li CH, van 't Erve OM, Robinson JT, Liu Y, Li L, Jonker BT. Electrical detection of charge-current-induced spin polarization due to spin-momentum locking in Bi2Se3. Nat Nanotechnol. 2014;9(3):218-24.
6. Guhr Th, A, Muller-Groening HA, Weiden M. Random matrix theories in quantum physics: common concepts. Physics report Vd. 1998;299:189-425.
7. Zhang T, Cheng P, Chen X, Jia JF, Ma X, He K et al. Experimental demonstration of topological surface states protected by time-reversal symmetry. Phys Rev Lett. 2009;103(26):266803.
8. Hsieh D, Qian D, Wray L, Xia Y, Hor YS, Cava RJ et al. A Topological Dirac insulator in a quantum spin Hall phase. Nature. 2008;452(7190):970-4.
9. Hasan MZ, Kane CL. Colloquium: Topological insulators. Rev Mod Phys. 2010;82(4):3045-67.
10. Chadov S, Qi X, Kübler J, Fecher GH, Felser C, Zhang SC. Tunable Multifunctional Topological Insulators in termary Heusler compounds. Nat Mater. 2010;9(7):541-5.
11. Lin H, Andre-Wray L, Yuqi X, Suyan X, Shuang J, Robert JC et al. Half-Heusler termary compounds as new multifunction experimental platforms for Topological quantum Phenomena. Nat Mater. 2010;9(7):546-9.
12. Hsieh D, Xia Y, Qian D, Wray L, Meier F, Dil JH et al. Observation of time-reversal-protected single-Dirac-cone topological-insulator states in Bi2Te and Sb2Te3; 2009.
13. Kane C, Moore J. Topological insulators. Physics world archive. IOP publishing Ltd;2014. ISSN: 0953-8585.
14. Naylor AJ. Towards highly-efficient thermoelectric power harvesting Gerators [Ph.D. thesis]. In: the Faculty of Natural and Environmental Sciences, School of Chemistry. University of Southampton; 2014.
15. Yang XX, Zhou ZF, Wang Y, Jiang R, Zheng WT, Sun CQ. Raman Spectroscopy Determination of the Debye temperature and Atomic Cohesive energy of CdS. CdSe, Bi2Se3 and Sb2Te3 nanostructure. J Appl Phys. Physical Review Letters. 2012;112(8):0835008.
16. Verma AS, Sarkar BK, Jindal VK. Cohesive Energy of Zincblende (AIIIBV and AIIBVI) Structured solids. Pramana J Phys. 2010;74(5):851-5.
17. Krumrain J, Mussler G, Borisova S, Stoica T, Plucinski L, Schneider CM, et al. MBE growth optimization of topological insulator Bi2Te3 films. J Cryst Growth. 2011;324(1): 115-8.
18. He HT, Wang G, Zhang T, Sou IK, Wong GK, Wang JN, et al. Impurity effect on weak antilocalization in the topological insulator Bi2Te3. Phys. Rev Lett. 2011;106 (16):166805.
19. Perdew JP, Wang Y. Accurate and simple analytic representation of the electron-gas correlation energy. Phys Rev B Condens Matter. 1992;45(23):13244-9.
20. Perdew JP, Burke K, Ernzerhof M. Generalized gradient approximation made simple. Phys Rev Lett. 1996;77:3865-8.
21. Abdu SG, Adamu MA, Onimisi MY. DFT computations of the ground state energy per atom of fullerenes (C60). Sci World J. 2018;13(1):35-8.
22. Galadanci GSM, Garba B. Computation of the Ground State Cohesive Properties of Alas Crystalline Structure Using FHI-aims code. IOSR-JAP. 2013;4(5):85-95.
23. Bernevig BA, Hughes TL, Zhang SC. Quantum spin Hall effect and topological phase transition in HgTe quantum wells. Science. 2006;314(5806):1757-61.
24. Kane CL, Mele EJ. Z2 topological order and the quantum spin Hall effect. Phys Rev Lett. 2005;95(14):146802.
25. König M, Wiedmann S, Brüne C, Roth A, Buhmann H, Molenkamp LW, et al. Quantum spin Hall insulator state in HgTe quantum wells. Science. 2007;318(5851): 766-70.
26. Giannozzi P. Density Functional Theory for electronic structure calculations structure della material. 2005;1.
27. Sholl DS, Steckel JA. Density functional theory: A practical introduction. John Wiley & Sons Inc Publication; 2009.
28. Tuckerman M 2004. Introduction to DFT. Maria Currie Tutorial Series. Modelling biomolecules.

29. Blum V, Gehrke R, Hanke F, Havu P, Havu V, Ren X et al. Ab iniotio molecular simulations with numeric atom-centered orbitals. Comput Phys Commun. 2009; 180(11):2175-96.
30. Burke K, Friends M. The ABC of DFT; 2008. Book Available on Line at htt://chem [cited 15/5/2018].
Available: http://ps.uci.edu/kieron/dft/book/.
31. Kohn W, Sham LJ. Self-consistent equations including exchange and correlation effects. Phys Rev. 1965;140 (4A):A1133-8.
32. Mishra SK, Satpathy S, Jepsen O. Electronic Structure and Thermoelectric Properties of bismuth telluride and bismuth selenide. J Phys: Condens Matter. 1997; 9(2):461-70.
33. Havu V, Blum V, Havu P, Scheffler M. Efficient O(N) integration for all-electron electronic structure calculation using numeric basis functions. J Comp Phys. 2009;228(22):8367-79.
34. Blum V, Gehrke R, Hanke F, Havu P, Havu V, Ren X et al. Ab initiomolecular simulations with numeric atom-centered orbitals. Comput Phys Commun. 2009;180 (11):2175-96.
35. Abdu SG, Adamu MA, Onimisi MY. DFT Computations of the lattice constant, stable atomic structure and the ground state energy per atom of fullerenes (c60). Sci World J. 2018;13(1).
ISSN 1597-6343
36. Viktor A, Oliver H, Sergey L. Hands-On Tutorial on ab initio Molecular Simulations, Tutorial I: Basics of Electronic-Structure Theory, Fritz-Haber-Institut der. Berlin: Max-Planck-Gesellschaft; 2011.
37. De Max-Planck-Gessellschaf B. Ab initio molecular simulations. Fritz Haber Institute (FHI aims). All-electron structure theory with numeric Atomcentered basis functions; 2011.
38. Francis A, Ahoume BA, Eli D. Cohesive energies calculation of gallium-arsenide and aluminium-arsenide: DFT study. J Niger Assoc Math Phys; 2017.
39. Abdu SG. Hartree-Fock Solutions of the hydrogen, helium, lithium, beryllium and Boron atoms. Niger J Phys. 2010; 21(2).
40. Kelly J. Magnetotransport of topological insulators: bismuth selenide and bismuth telluride. National Stroke Foundation/REU Program, Physics Department, University of Notre Dame; 2011.

Peer-review history:
The peer review history for this paper can be accessed here:
https://www.sdiarticle5.com/review-history/88040